Chemical and biological activity in three-dimensional flows

Alessandro P. S. de Moura* and Celso Grebogi
Instituto de Física, Universidade de São Paulo, Caixa Postal 66318, 05315-970, São Paulo, São Paulo, Brazil
(Received 28 April 2003; revised manuscript received 25 May 2004; published 30 August 2004)

We study the dynamics of active particles advected by three-dimensional (3D) open incompressible flows, both analytically and numerically. We find that 3D reactive flows have fundamentally different dynamical features from those in 2D systems. In particular, we show that the reaction's productivity per reaction step can be enhanced, with respect to the 2D case, while the productivity per unit time in some 3D flows goes to zero in the limit of high mixing rates, in contrast to the 2D behavior, in which the productivity goes to a finite constant. These theoretical predictions are validated by numerical simulations on a generic map model.

DOI: 10.1103/PhysRevE.70.026218 PACS number(s): 05.45.−a, 47.70.−n, 47.70.Fw, 47.52.+j

In the last few years, there has been great interest in the dynamics of active particles advected by open chaotic flows [1]. Activity includes chemical activity, when reacting molecules are consumed in a chemical process to yield product molecules; and also biological activity, when, for instance, a unicellular organism makes copies of itself after taking in food. There is a host of important physical and environmental processes involving active flows, including the depletion of the ozone layer [2], the dynamics of pollutants in the atmosphere [3], plankton population dynamics in the ocean [4,5], early life evolution [6], and others. All these can be considered open systems, because the region where activity takes place (the interaction region) is much smaller than the whole system.

The advection of particles by open chaotic flows displays the phenomenon of chaotic scattering [7,8]. A chaotic scattering dynamics is characterized by the presence of a fractal invariant set of nonescaping unstable orbits [9]. This set is called the chaotic saddle. It is known that the presence of a chaotic saddle in the advection dynamics has dramatic effects on the reactive dynamics. These and other studies up to now refer to two-dimensional (2D) flows. However, actual flows are three dimensional, and only under artificial restrictions are they reasonably approximated by two-dimensional models. Therefore, the full three-dimensional dynamics must be taken into account in order to successfully understand activity in realistic flows [15].

In this article, we develop a theory for the dynamics of reactive particles in open hyperbolic (and, hence, generic) three-dimensional flows. We find striking differences from the corresponding results for 2D flows, showing that the 3D character of the dynamics must not be disregarded. To simplify the analysis of the different dynamical features found in the 3D flows, we assume the flow to be periodic in time. In this case, the dynamics can be reduced to a 3D volume-preserving map with escapes (since we are dealing with open flows). Because of its odd dimensionality, the number of stable directions of the dynamics is different from the number of unstable ones: such maps are not Hamiltonian, even though they preserve the three-dimensional volume. Since volume is preserved, there are two nondegenerate cases of hyperbolic 3D flows: those having one unstable and two stable directions (we call these "type I"), and those with two unstable and one stable directions (we call these "type II"). To investigate the reaction dynamics in 3D flows, we develop an analytic model. We show that the reacting particles concentrate along the chaotic saddle's unstable manifold. For scales larger than the particle size, the distribution looks like a fractal, with a fractal dimension equal to that of the unstable manifold. We show that the two types of dynamics (type I and type II) correspond to very distinct types of reaction dynamics. In particular, our theory predicts that the production term in the reaction equation in the continuum limit is proportional to A^{γ}, where A is the amount of reactant, and γ is a coefficient that depends on the fractal dimension of the unstable set. For type I flows, we show that γ can be positive, whereas in the 2D case it is always negative. In this case, the reaction kinetics of the 3D flow is qualitatively different from that of the 2D flow. In particular, we show that the reaction's productivity *per reaction step* can be enhanced in type I flows with respect to the 2D case, while the productivity *per unit time* in some 3D flows goes to zero in the limit of high mixing rates, in contrast to the 2D behavior, in which the productivity goes to a finite constant. We generally find that within the 3D case type I and type II flows have very distinct reaction dynamics, with type II flows behaving in most respects like 2D flows, whereas type I flows display many unusual features. These results must be taken into account when studying the active dynamics of more realistic systems.

We first present results on the purely advective dynamics of a 3D flow, without considering activity for the time being. We study the case of a time-periodic flow, the dynamics of which can be reduced to a 3D stroboscopic map, as is usually done in dynamical systems. In order that our results do not depend on the particularities of the chosen model, we choose to focus on a generic hyperbolic open volume-preserving 3D map, which can be thought of as a generalization of the well-known 2D open baker map. The structural stability of our map rigorously guarantees that our results are generic, for a large class of 3D flows (3D volume-preserving maps for closed systems have been studied before [10]). The map is defined in the unit *xyz* cube, and its action is shown in Fig. 1(a). We denote the map by $\mathcal{M}$. One iteration of $\mathcal{M}$ consists

*Email address: amoura@if.usp.br

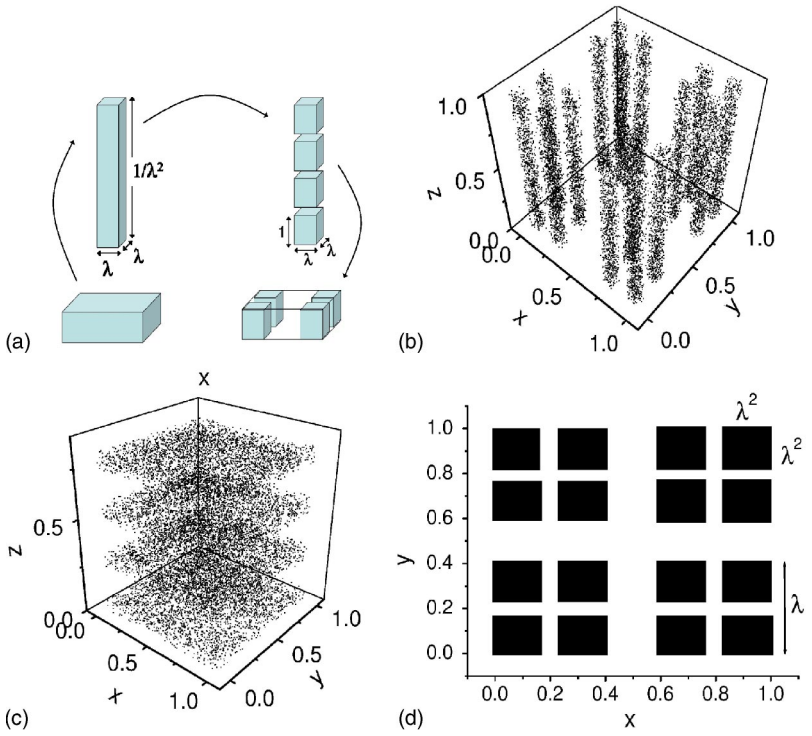

FIG. 1. (a) Illustration of the action of one iteration of map $\mathcal{M}$ on the unit cube (the drawing is not to scale). (b) Surviving points after two iterations of the map $\mathcal{M}$, for $\lambda=0.35$, with initial conditions chosen randomly in the cube. (c) Same as (a), but for the inverse map $\mathcal{M}^{-1}$. (d) Intersection with a horizontal plane ($z=$const) of the set of surviving points after two iterations of $\mathcal{M}$.

of two actions. First, the x and y directions are uniformly contracted by a factor λ, with $\lambda<1/2$, while the z direction undergoes an expansion by a factor $1/\lambda^2$, thereby conserving volume. By this transformation, the unit cube turns into a long thin parallelepiped with its long axis along the z axis. Second, four pieces with unit height of this parallelepiped are selected and put in the four corners of the cube (see Fig. 1). The pieces of the parallelepiped that are not selected are discarded, and considered to have escaped. Formally, $\mathcal{M}$ is written as

$$\mathcal{M}:\begin{cases} x_{n+1}=\lambda x_n + B_x, \\ y_{n+1}=\lambda y_n + B_y, \\ z_{n+1}=z_n/\lambda^2 + B_z, \end{cases} \tag{1}$$

where the additive factors B depend on the value of z_n:

$$B_x=B_y=0 \ \text{ if } \ 0\leqslant z_n<1,$$

$$B_x=1-\lambda,\ B_y=0,\ B_z=-C \ \text{ if } \ C\leqslant z_n<C+1,$$

$$B_x=1-\lambda,\ \ B_y=0,\ B_z=-C \ \text{ if } \ 2C\leqslant z_n<2C+1,$$

$$B_x=B_y=1-\lambda,\ B_z=-3C \ \text{ if } \ 3C\leqslant z_n<3C+1, \tag{2}$$

with $C=(2\lambda)^{-2}$. We could have defined the map more generally, with two distinct contraction factors λ_x and λ_y. The general conclusions would be the same.

The map $\mathcal{M}$ described by Eq. (1) has two contracting directions and one expanding direction, and is therefore of type I. We observe that for the inverse map $\mathcal{M}^{-1}$, stable directions turn into unstable ones, and vice versa. Therefore, $\mathcal{M}^{-1}$ has one stable and two unstable directions, and it is of type II. We thus conveniently handle the two generic types of hyperbolic 3D maps with one single map and its inverse.

From Eq. (1) [see Fig. 1(a)], the stable manifold of $\mathcal{M}$ is a Cantor set of planes parallel to the xy plane, and the unstable manifold is a Cantor set of vertical segments. We can visualize these manifolds by iterating $\mathcal{M}$ forward a given number of times for many initial conditions chosen randomly within the unit cube and plotting the points that have not escaped. Conversely, iterating $\mathcal{M}$ backward gives a picture of the stable manifold of $\mathcal{M}$. The results are shown in Figs. 1(b) and 1(c).

Let us consider now the unstable manifold of $\mathcal{M}$, depicted in Fig. 1(b). Since it is made up of vertical segments, and since the expansion and contraction rates are uniform, we can restrict ourselves to the intersection of the unstable manifold with a horizontal plane. This is depicted in Fig. 1(d). In the limit of an infinite number of iterations, a well-known Cantor set in the plane is formed [11], with fractal (box-counting) dimension given by $\bar{d}=-2\ln 2/\ln\lambda$. The unstable set is the product of this set and a one-dimensional segment, with dimension

$$d_u=1-2\ln 2/\ln\lambda. \tag{3}$$

Note that d_u is also the dimension of the *stable* manifold of $\mathcal{M}^{-1}$. A similar reasoning can be applied to the stable manifold: it is the product of a Cantor set on a vertical line with a plane. We find $d_s=2-\ln 2/\ln\lambda$. The chaotic saddle is the intersection of the stable and unstable manifolds, and its dimension is $d_{saddle}=-3\ln 2/\ln\lambda$. We see from the above that $d_u\neq d_s$, in contrast to the 2D case. Furthermore, d_s and d_u satisfy

$$1<d_u<3,\ 2<d_s<3. \tag{4}$$

We note that the structure of the stable and unstable manifolds of the two types of flow for a generic open 3D volume-

preserving map [and not only for map (1)] is topologically similar to that shown in Fig. 1. Also, the inequalities (4) hold in general.

We observe from Eq. (4) that in type II flows the dimension of the stable manifold [which is d_u in Eq. (4)] may be less than 2. In this case, the stable manifold has generically a null intersection with a one-dimensional curve, and thus a 1D scattering function (such as the escape time) is smooth, even though there is a fractal invariant set. If $d_u > 2$, on the other hand, a typical scattering function has a fractal set of singularities [9]. This is a phenomenon analogous to the one found in Hamiltonian chaotic scattering in three-degree-of-freedom systems [12,13]. The transition point, at which $d_u = 2$, is given by $\lambda = \lambda_c = 1/4$. If the fluid is of type II, however, this transition does not occur.

We now consider what happens when the advected particles are active. We first derive an analytical model valid for general hyperbolic 3D flows, and then we will use the map (1) to corroborate our results. Reactions are implemented by a discretization of space, following [14]. We initially choose a region R of space that contains the chaotic saddle, and which we consider to be the interaction region. We then partition R into cubic cells of size σ, which physically represents the reaction range or the particle size. Each of the advected active particles is located in one of the cells. For a given particle in an arbitrary position in R, we consider it to be localized at the center of the cell that contains it. When it evolves in time through a 3D map, this particle is mapped to another cell. If the mapping takes a particle outside R, it is considered to have escaped. If two particles are mapped to the same cell, only one is considered to remain (coalescence). After advection, the particles undergo a sudden reaction. We assume that all particles undergo a catalytic reaction, which acts as an infection: if a given cell contains a particle before the reaction, all neighboring cells will also contain particles after the reaction. If an infected cell already has a particle, it remains unaltered. The total dynamics of the system is thus composed of advection and reaction. To fully define the dynamics, we have to specify the reaction time τ. The reaction rate is given by $1/\tau$. We assume τ either to be an integer m (the map is iterated m times before the reaction takes place) or to take values of the form $1/m$ (reaction takes place m times in each iteration). The continuous time limit is obtained by letting σ, $\tau \to 0$ while keeping the reaction velocity $v_R = \sigma/\tau$ finite.

We consider first type I flows, with one unstable direction. Let $A_0(n)$ denote the volume of cells occupied by reacting particles right after the nth reaction. Similarly, $A_\tau(n)$ is the reactants' volume right before the $(n+1)$th reaction. They are related by $A_\tau(n) = e^{-\nu} A_0(n)$, where $\nu = \kappa\tau$ is the decay rate, and κ is the escape rate by advection. For $\mathcal{M}$, κ is given by $e^{-\kappa} = 4\lambda^2$. Due to the stretching along the unstable direction, the particles rapidly accumulate into filaments about the Cantor set of curves that makes up the unstable manifold. The volume A is given in terms of the average width ε of the filaments by

$$A_\tau(n) = \mathcal{H}[\varepsilon_\tau(n)]^{3-d_u}, \tag{5}$$

where the same notational conventions used for A hold for ε, and $\mathcal{H}$ is the Hausdorff measure of the unstable manifold [11].

When reactions occur, the filaments are thickened by approximately σ, yielding $\varepsilon_0(n+1) = \varepsilon_\tau(n) + \alpha\sigma$, where α is a geometric factor that takes the curvature and overlapping of the filaments into account. We are assuming that no new reacting particles are entering the system from the outside, and that the only source of new particles is the reaction itself. Using this relation together with Eq. (5), we can write an equation for the discrete time evolution of the volume:

$$A_\tau(n+1) = e^{-\nu}\{[A_\tau(n)]^{1/(3-d_u)} + \sigma g\}^{3-d_u}, \tag{6}$$

with $g = \alpha\mathcal{H}^{1/(3-d_u)}$. By requiring $A_\tau(n+1) = A_\tau(n) = A_\tau^*$, we find the equilibrium value of A_τ:

$$A_\tau^* = \left[\frac{\sigma g}{e^{\nu/(3-d_u)} - 1}\right]^{3-d_u}. \tag{7}$$

From Eq. (7) we see that A_τ^* scales with σ as $A_\tau^* \sim \sigma^{3-d_u}$. To verify this prediction, we simulate the advection-reaction dynamics of map (1). Figure 2(a) shows the number of particles N as a function of σ for one value of λ. Equation (7) predicts that $N \sim \sigma^{-d_u}$. This is confirmed by numerical fitting of the data of Fig. 2(a).

In the continuous limit, A is a continuous function of space and time. By Taylor-expanding Eq. (6), we get a differential equation for A, the reaction kinetic equation

$$dA/dt = -\kappa A + g(3 - d_u) v_R A^\gamma, \tag{8}$$

where the coefficient of the power law is $\gamma = (2 - d_u)/(3 - d_u)$. The first term in Eq. (8) is due to the escape, and the second term is the source term, which depends on the geometry of the unstable manifold. If $d_u > 2$, then $\gamma < 0$, whereas if $d_u < 2$, $\gamma > 0$. In the two-dimensional case, only the case $\gamma < 0$ is possible, and the source term in Eq. (8) is singular and diverges for $A \to 0$, giving rise to the so-called dynamical catalysis [14]. The case $\gamma > 0$ is uniquely three dimensional, with no counterpart in 2D flows. In this case the source term vanishes as $A \to 0$. In the case of our map (1), the crossing point between the two behaviors is at $\lambda = \lambda_c = 1/4$, the same at which scattering functions of $\mathcal{M}^{-1}$ become fractal. This transition can be understood from the behavior of the area of the two-dimensional boundary separating the region filled with particles from the region devoid of particles. This area determines the efficiency of the dynamical catalysis. It can be shown that in the limit as $A \to 0$ this area vanishes when $d_u < 2$, and it diverges when $d_u > 2$.

To understand better the consequences of this transition from $\gamma < 0$ to $\gamma > 0$, we turn our attention to the production P per reaction step, defined as the difference between $A_0(n+1)$ and $A_\tau(n)$, after dynamical equilibrium is reached. It is straightforward to show that $P = (e^\nu - 1)A_\tau^*$ [14]. In Fig. 2(b), the dependence of P on ν is plotted for both $d_u < 2$ and $d_u > 2$. For $\nu \ll 1$, from Taylor expansion, we find that P scales as

$$P \sim \nu^{d_u - 2}. \tag{9}$$

From the above, in the limit $\nu \to 0$, or equivalently for $\tau \to 0$ (high reaction rate), $P \to 0$ if $d_u > 2$, and $P \to \infty$ if $d_u < 2$. Thus, $d_u = 2$ separates two very different dynamical regimes. We emphasize that this occurs only in 3D flows.

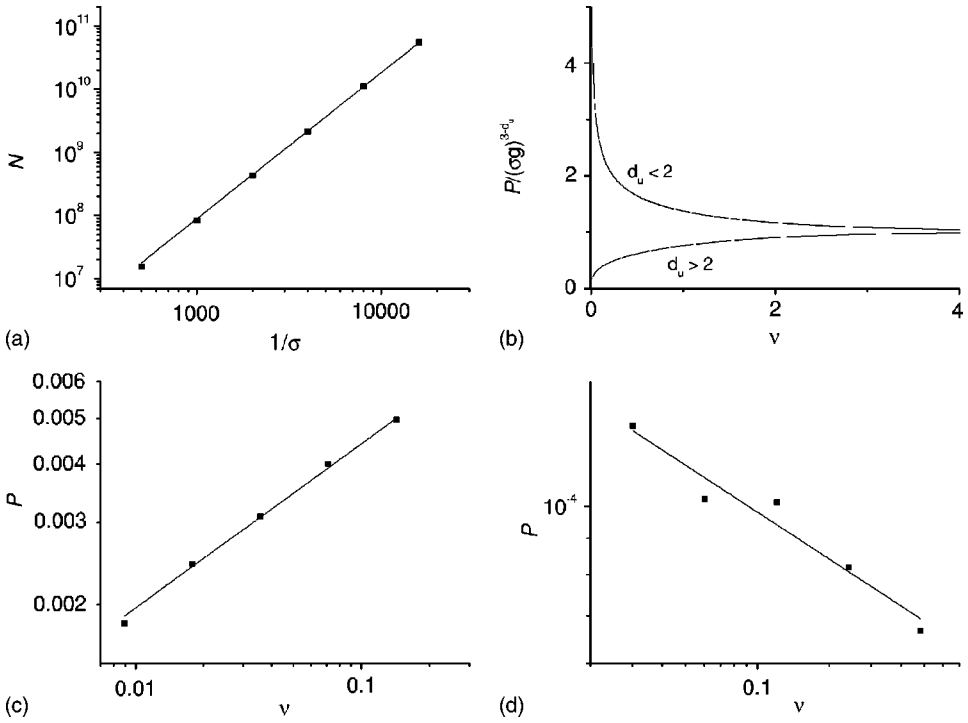

FIG. 2. (a) Number N of occupied cells in the equilibrium distribution as a function of the inverse of the grid size σ, for $\lambda=0.35$; from the slope we get a dimension $d_u=2.31\pm0.01$, which agrees with the theoretical value $d_u=2.32$ obtained from Eqs. (3). (b) Plot of the ν-dependent part of the theoretical production P, for $\lambda=0.15$ (upper curve) and $\lambda=0.35$ (lower curve). (c) Production obtained from simulation, as a function of ν, for $\lambda=0.35$, that is, for $d_u>2$; the slope gives $P\sim\nu^{0.35\pm0.02}$, which compares well with the theoretical value 0.32 of the coefficient, from Eqs. (3) and (9). (d) Same as (c), with $\lambda=0.15$ and $d_u=1.73<2$; the slope gives a power law with a coefficient -0.23 ± 0.04, which is close to the theoretical value of -0.27.

We verified Eq. (9) through simulation, as is shown in Figs. 2(c) (for $d_u>2$) and 2(d) (for $d_u<2$), where P is calculated for several values of ν for the map (1). The power-law relation predicted by Eq. (9) is verified quantitatively, to within numerical errors. There is thus an enhancement of the reaction's productivity per reaction step as $\nu\to0$, which is an exclusively three-dimensional phenomenon, and which is not found in 2D flows.

The same derivation can be applied, with practically no changes, to type II flows. Type II flows, however, have an unstable manifold dimension which is always greater than 2 [from Eq. (4)] and therefore behave like 2D flows.

Another important quantity is the productivity Q per unit time, which is the amount of new reactant produced in one time unit. For type I flows, in the continuous time limit and in equilibrium, $Q=\kappa A^*$, with A^* given by the nontrivial equilibrium solution ($dA/dt=0$) of Eq. (8). We thus get

$$Q=\kappa A^*=(g(3-d_u)v_R)^{3-d_u}\kappa^{d_u-2}. \tag{10}$$

Q is the productivity in unit time only in the limit of continuous time reactions, that is, for $\tau\to0$.

In the above expression, d_u is a function of κ. In fact, using Eq. (3) and the expression $\exp(-\kappa)=4\lambda^2$, we can eliminate λ, and find d_u as a function of κ. The result is

$$d_u=\frac{\kappa+6\ln2}{\kappa+2\ln2}. \tag{11}$$

Substituting this expression in Eq. (10), we get Q directly as a function of κ:

$$Q=\left(\frac{2gv_R\kappa}{\kappa+2\ln2}\right)^{\eta}\kappa^{(2\ln2-\kappa)/(\kappa+2\ln2)}, \tag{12}$$

where $\eta=2\kappa/(\kappa+2\ln2)$. In the limit of high escape rate ($\kappa\to\infty$), we get

$$Q\to(2gv_R)^2\kappa^{-1}. \tag{13}$$

Thus, as $\kappa\to\infty$, the production in unit time decreases to zero as $1/\kappa$, in the case of a type I 3D flow (with two contracting directions).

In the case of 2D flows, instead of Eq. (10) we have the following equation for the production per unit time:

$$Q=[g(2-d_u)v_R]^{2-d_u}\kappa^{d_u-1}. \tag{14}$$

For the 2D baker map, the relation between d_u and κ is given by $d_u=(\kappa+2\ln2)/(\kappa+\ln2)$, and in the limit of $\kappa\to\infty$, we get

$$Q\to(2gv_R)^2\kappa^{\ln2/\kappa}. \tag{15}$$

Therefore, in the limit of high escape rate, $Q\to(2gv_R)^2$ (since $\kappa^{1/\kappa}\to1$ for $\kappa\to\infty$). In 2D flows, the production per unit time goes to a finite limit, in contrast to the type I 3D case, where it goes to zero. This is an important difference between the two regimes. We note that in this respect type II 3D flows (with two expanding directions) behave in the same way as a 2D flow. Again, we have a qualitatively different behavior for the 2D and 3D dynamics.

We conclude by commenting on how the above theory is related to realistic environmental flows. An isolated ocean island is a barrier to ocean currents, and a wake is formed behind the island. This wake corresponds to the interaction region, and the flow can be considered open, because this interaction region is much smaller than the ocean as a whole. According to our results, active processes undergone by par-

ticles carried by the water (for instance, reproducing plankton or chemical reactions by pollutants) will depend on whether the flow is type I or type II, and on the value of the unstable dimension d_u. This in turn depends on the boundary conditions of the flow, and has to be ascertained for each case. This is quite independent of the particulars of the reaction. Similar considerations apply to the atmosphere and the wake behind an isolated mountain.

This work was supported by FAPESP and CNPq.

[1] See the Chaos **12**, 372 (2002), special issue on active chaotic flows.
[2] D. G. H. Tan *et al.*, J. Geophys. Res., [Atmos.] **103**, 1585 (1998);A. Mariotti *et al.*, J. Atmos. Sci. **57**, 402 (2000).
[3] Z. Liu, Y.-C. Lai, and J. M. Lopez, Chaos **12**, 417 (2002).
[4] G. Károlyi *et al.*, Proc. Natl. Acad. Sci. U.S.A. **97**, 13 661 (2000).
[5] Z. Neufeld, C. López, and P. H. Haynes, Phys. Rev. Lett. **82**, 2606 (1999);Z. Neufeld *et al.*, Phys. Rev. E **61**, 3857 (2000).
[6] G. Károlyi, I. Scheuring, and T. Czárán, Chaos **12**, 460 (2002).
[7] D. J. Tritton, *Physical Fluid Dynamics* (Oxford University Press, Oxford, 1988).
[8] E. Zemniak, C. Jung, and T. Tél, Physica D **36**, 123 (1994).
[9] T. Tél, in *Directions in Chaos*, edited by H. Bai-Lin (World Scientific, Singapore, 1996).
[10] M. Feingold, L. P. Kadanoff, and O. Piro, J. Stat. Phys. **50**, 529 (1988);O. Piro and M. Feingold, Phys. Rev. Lett. **61**, 1799 (1988).
[11] K. J. Falconer, *The Geometry of Fractal Sets* (Cambridge University Press, Cambridge, U.K., 1986).
[12] Y.-C. Lai, A. P. S. de Moura, and C. Grebogi, Phys. Rev. E **62**, 6421 (2000).
[13] Q. Chen, M. Ding, and E. Ott, Phys. Lett. A **145**, 93 (1990);D. Sweet, E. Ott, and J. A. Yorke, Nature (London) **399**, 315 (1999).
[14] Z. Toroczkai *et al.*, Phys. Rev. Lett. **80**, 500 (1998); G. Károlyi *et al.*, Phys. Rev. E **59**, 5468 (1999).
[15] Tuval *et al.*, Europhys. Lett. **65**, 633 (2004).